Photophysical, Electrochemical, and Electrogenerated Chemiluminescent Properties of 9,10-Dimethyl-7,12-diphenylbenzo[*k*]fluoranthene and 9,10-Dimethylsulfone-7,12-diphenylbenzo[*k*]fluoranthene†

Eve F. Fabrizio, Andrew Payne, Neil E. Westlund, Allen J. Bard,* and Philip P. Magnus

Department of Chemistry and Biochemistry, University of Texas at Austin, Austin, Texas 78712

Received: May 24, 2001; In Final Form: October 22, 2001

A newly synthesized light emitting compound 9,10-dimethylsulfone-7,12-diphenylbenzo[*k*]fluoranthene (DSDPBF) and its synthetic intermediate 9,10-dimethyl-7,12-diphenylbenzo[*k*]fluoranthene (DMDPBF) were studied to evaluate how the addition of weak electron donating methyl groups and the subsequent addition of an electron withdrawing sulfone group affect the photophysical and electrochemical properties as well as the rate of radical cation coupling of the parent compound, 7,12-diphenylbenzo[*k*]fluoranthene (DPBF). Although the photochemical and electrochemical properties of DSDPBF were more similar to the unsubstituted DPBF than to the DMDPBF, there was a substantial decrease in the quantum efficiency upon addition of the electron-rich sulfone group which was not observed upon addition of the methyl groups. On the other hand, the rate of radical cation coupling or dimerization observed upon electrochemical oxidation varied significantly. The addition of the electron donating methyl groups decreased the reactivity of the radical cation resulting in a 40 times slower rate of dimerization than that observed for the unsubstituted benzo[*k*]fluoranthene, whereas the addition of the electron withdrawing sulfone group to the methyl groups increased the radical cation reactivity resulting in a rate of dimerization that was 3 times faster than the unsubstituted parent compound. As a result, the electrogenerated chemiluminescence emission spectrum obtained from the annihilation reaction between the radical anion and radical cations of DSDPBF was dominated by emission from the dimer at 589 and 621 nm instead of emission from the monomer at ca. 485 nm.

Introduction

Electron transfers between oppositely charged radical ions can produce electronically excited products that, under the appropriate conditions, emit light.[1] This process, when it occurs at an electrode, is called electrogenerated chemiluminescence (ECL) and can occur by either subsequent ion-annihilations or through the use of highly energetic radical co-reactants.[2] Research involving ECL has focused on a number of areas. One area of rapid development is the design of new, more efficient electroluminescent compounds for potential use in organic light emitting diodes (OLEDs). A second involves the development of multiple wavelength labels to facilitate simultaneous ECL detection in bio-analytical assays. Within the past few years, our group has been synthesizing and investigating new light-emitting compounds based on variations in the structure of 7,-12-diphenylbenzo[*k*]fluoranthene (DPBF).[3] This recently developed synthetic route allows us to readily alter the structure of DPBF making this an ideal means for evaluating the effects of increased conjugation and of added substituents on the photophysical properties, in particular, quantum efficiency and emission wavelength.

A new light emitting compound, 9,10-dimethylsulfone-7,12-diphenylbenzo[*k*]fluoranthene (DSDPBF; **11**), and its intermediate, 9,10-dimethyl-7,12-diphenylbenzo[*k*]fluoranthene (DMDPBF; **8**), have been synthesized. The overall synthetic mechanism is presented in Schemes 1 and 2. Although the sulfone group was added to facilitate further reactivity with alkyne-containing groups through a heat activated Diels−Alder reaction, we were also interested in examining the effects of this electron withdrawing substituent on the photophysical and electrochemical properties of benzo[*k*]fluoranthene. The optimized molecular geometry using AM1 semiempirical calculations is given in Figure 1. As is evident by this structure, both phenyl groups as well as the oxygens of the sulfone are almost perpendicular to the planar aromatic benzo[*k*]fluoranthene. Even though the

SCHEME 1

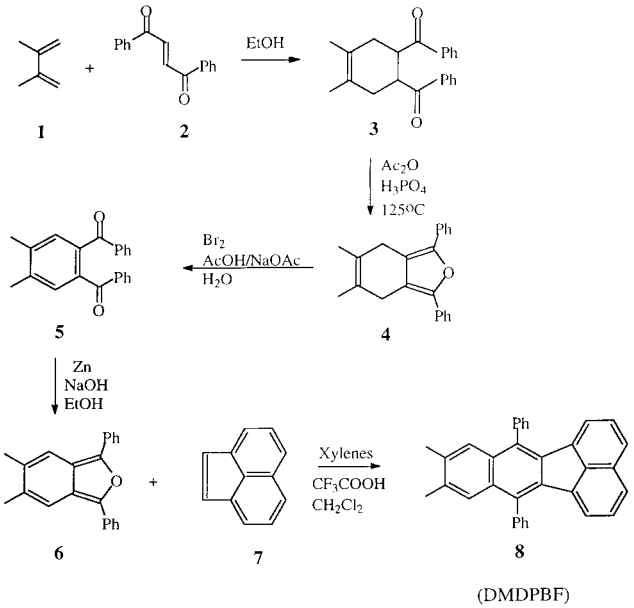

† Part of the special issue "Noboru Mataga Festschrift".

* To whom correspondence should be addressed.

10.1021/jp012012s CCC: $22.00
Published on Web 12/06/2001

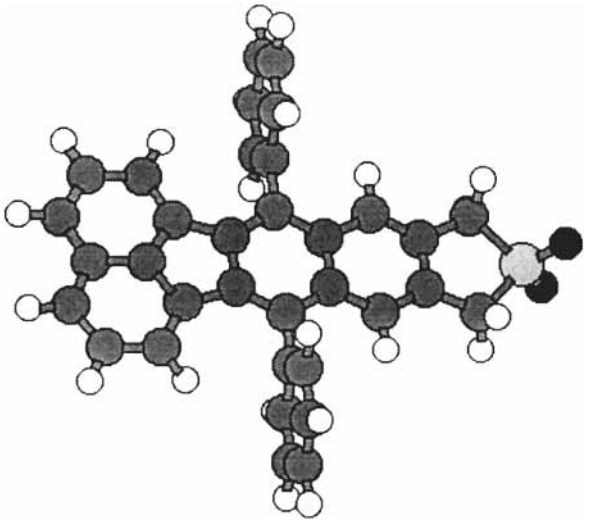

Figure 1. Optimized geometry for DSDPBF as determined from AM1 semiempirical calculations.

SCHEME 2

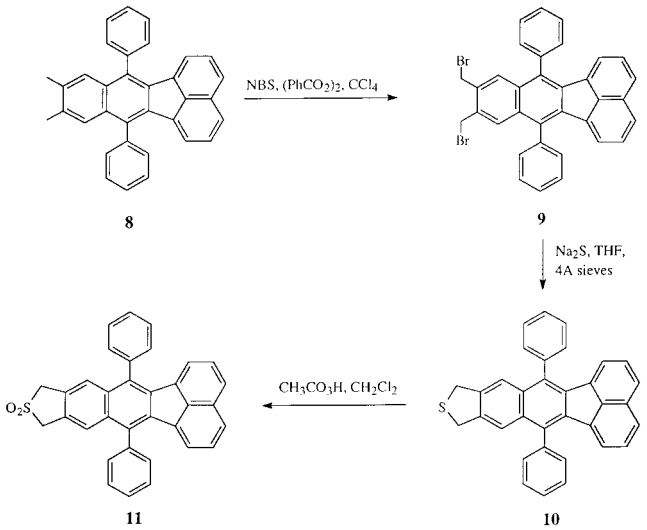

(DSDPBF)

sulfone group is electron withdrawing, this group is positioned one carbon from the aromatic π system on benzo[*k*]fluoranthene and, therefore, would be expected to have little or no effect on the spectroscopic and electrochemical properties of this compound relative to the previously studied unsubstituted diphenylbenzo[*k*]fluoranthene.

Additionally, we are interested in how the electron donating methyl groups and the addition of the electron withdrawing sulfone group to these methyl groups affect the chemical reactivity of benzo[*k*]fluoranthene upon oxidation. In our previous studies, DPBF was determined to undergo two relatively fast radical cation−radical cation couplings (RRCs) upon electrochemical oxidation to produce a longer wavelength emitting dimer.[3a] The overall reaction is given in Scheme 3. Scan rate studies of the unsubstituted DPBF as well as theoretical simulations determined the rate of dimerization to be 7500 $M^{-1}s^{-1}$. One would expect this rate to decrease upon stabilization of the radical cations with the addition of an electron donating group and to increase with the addition of an electron withdrawing group onto benzo[*k*]fluoranthene; however, in the case of dimethyl sulfone, the electron withdrawing group is positioned one carbon away from the aromatic core structure making it difficult to predict an effect on radical cation coupling.

SCHEME 3

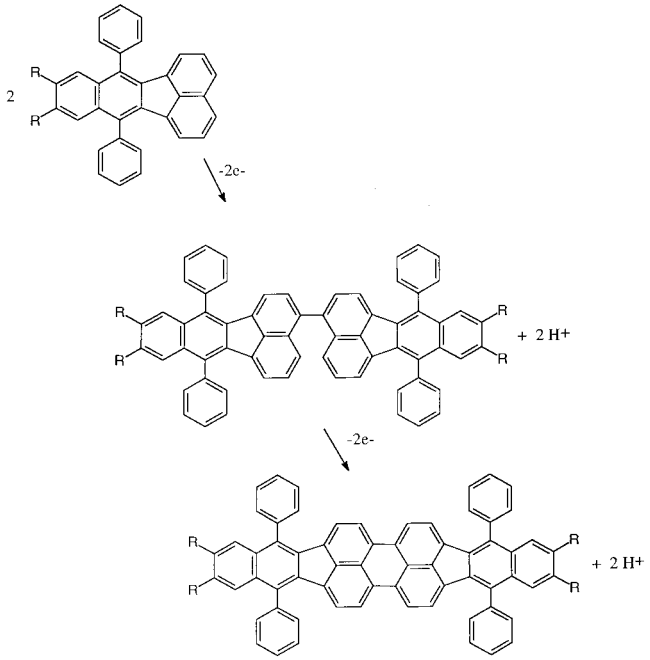

We present here the effect on the photophysical and electrochemical properties of DPBF by the addition of weak electron-donating methyl groups (**8** in Scheme 1), an intermediate in the overall synthesis, as well as the subsequent addition of the electron withdrawing group, sulfone (**11** in Scheme 2), to the 9 and 10 positions of benzo[*k*]fluoranthene. These results provide further insight into the future development of compounds for ECL using variations of the core benzo[*k*]fluoranthene structure.

Experimental Section

Materials. Tetra-*n*-butylammonium hexafluorophosphate ($TBAPF_6$; SACHEM, Inc., Austin, TX) was recrystallized three times from $EtOH/H_2O$ (4:1) and dried in a vacuum oven at 100 °C for 4 h prior to use. Diphenylanthracene (Aldrich) was recrystallized from absolute ethanol prior to use. Benzene (Aldrich, ACS grade) and acetonitrile (CH_3CN; Burdick and Jackson, UV grade) were used as received after being transferred unopened into an inert atmosphere drybox (Vacuum Atmospheres Corp.). Rubrene (Sigma Chemical Co.) was used as received and transferred open into the inert atmosphere drybox. All fluorescence, electrochemical, and ECL solutions were prepared inside the drybox containing helium and sealed in the appropriate airtight cells for measurement. UV−vis measurements were taken from the same solutions used to obtained the electrochemical and fluorescence measurements.

Spectroscopy. All fluorescence spectra were recorded on an ISA Spex Fluorolog-3 (JY Horiba, Edison, NJ) with excitation and emission slit widths set at 0.5 nm and a resolution of 1 nm. All absorbance spectra were obtained with a Milton Roy Spectronic 3000 Array spectrophotometer with a resolution of 0.4 nm. The absorbance and fluorescence spectra of monomers of DMDPBF and DSDPBF and the dimer of DMDPBF were obtained in pure benzene at a concentration of 19.9 μM. The relative fluorescence efficiency of the monomers was determined using diphenylanthracene (DPA) (λ_{ex} = 380 nm, ϕ_{DPA} = 0.91 in benzene) as a standard, whereas the fluorescent efficiency of the DMDPBF ladder dimer was determined using rubrene (λ_{ex} = 500 nm, $\phi_{rubrene}$ = 0.98 in benzene) as standards.[4]

Electrochemistry. Electrochemical measurements were recorded with a CH Instruments model 660 Electrochemical

Workstation (Austin, TX). The working electrode consisted of a platinum disk either 1 or 3 mm in diameter inlaid in glass. All electrodes were polished with 0.05 μm alumina (Buehler, Ltd.) and sonicated in water and then in ethanol for 5 min each and then dried in an oven at 110 °C for 10 min. A platinum coil served as the counter electrode, and a silver wire contained in a separate compartment containing a Vycor glass frit (BAS, West Lafayette, IN) served as a quasi-reference-electrode. Concentrations of DMDPBF and DSDPBF varied depending on the electrochemical experiment but ranged from 1 to 3 mM. All standard potentials are versus SCE and were determined by adding ferrocene (taking $E^{o}_{Fc/Fc+} = 0.424$ V vs SCE in benzene) as an internal potential marker.[3]

Bulk electrolysis to produce the dimer was performed using a large area platinum mesh working electrode and a large area platinum mesh counter electrode that was placed in a compartment that was separated from the working electrode by a fine glass frit. The reference electrode consisted of a silver wire placed in the same compartment as the working electrode but separated by glass frit made of Vycor. The working electrode was biased 1.6V vs Ag wire for 1 h using a Princeton Applied Research (PAR, Princeton, NJ) model 175 universal programmer, model 173 potentiostat−galvostat, and model 179 digital coulometer.

Calculations. Semiempirical AM1 calculations were performed using HyperChem (HyperCube, Inc., Gainesville, FL). The following molecular parameters were used: total charge was set to zero, the spin multiplicity was one, the iteration limit was 50, the convergent limit was 0.01, the spin pairing was set to RHF, and the lowest state was determined. The optimized geometry in vacuo was determined by using the Fletcher−Reeves algorithm with termination conditions consisting of a RMS gradient of 0.05 Kcal/A mol or a total of 1680 cycles.

Electrogenerated Chemiluminescence. ECL measurements were obtained using the same procedure as previously reported.[5] These measurements were made with solutions prepared in the same manner as those used to obtain the cyclic voltammograms. The working electrode in all cases was a platinum disk approximately 3 mm in diameter inlaid in glass. The concentration for the monomers of DMDPBF and DSDPBF were approximately 2 ± 0.2 mM, whereas the concentration for the dimer of DMDPBF was 0.5 ± 0.1 mM as the result of low solubility in the solvent mixture. The cell was pulsed between the oxidation and reduction peak potentials of each compound using a Princeton Applied Research (PAR, Princeton, NJ) model 175 universal programmer, model 173 potentiostat−galvostat, and model 179 digital coulometer. The pulse width for all experiments was 0.1 s. All spectra were recorded using a charge couple device (CCD) camera (Photometrics CH260, Photometrics, Tucson, AZ) cooled to −100 °C and a Chemspec 100S (American Holographic, Littleton, MA) spectrometer. The relative ECL efficiencies were determined using $Ru(bpy)_3(ClO_4)_2$ as the standard ($\phi_{ECL} = 0.05$). The apparatus and methodologies for determining the ECL efficiency have been previously published.[5]

Synthesis of DMDPBF (8). The overall reaction mechanism that was used to synthesize this compound is shown in Scheme 1. The first five steps are similar to the previously reported synthesis of DPBF.[3] A solution of isobenzofuran (**6**; 1.10 g, 3.68 mmol, 1.0 equiv) and freshly sublimed acenaphthylene (**7**; 0.671 g, 4.41 mmol, 1.2 equiv) in xylenes (18 mL) was heated to reflux under argon. After 17 h, the solution was allowed to cool to room temperature; some precipitate appeared in the solution at this time. Removal of the solvent by distillation under reduced pressure afforded and an orange-yellow solid which was shown by ^{1}H NMR to be a 1:1 mixture of exo:endo adducts. The solid was dissolved in anhydrous acetonitrile (CH_2Cl_2; 18 mL) and anhydrous trifluoroacetic acid (1.8 mL). The mixture was heated at reflux under argon for 20 h and then allowed to cool to room temperature. Removal of the solvent by distillation under reduced pressure and azeotropic distillation of the trifluoroacetic acid with ethyl acetate (EtOAc) produced a beige solid. Flash column chromatography over silica gel, eluting with 2% ether−hexane, afforded dimethyldiphenylbenzo[*k*]fluoranthene (**8**) as a fluorescent yellow solid (1.40 g, 88%): R_f 0.45 (2% ether-benzene); mp 265−270 °C (decomposes); ν_{max} (film) 3056, 2916, 1593, 1494, 1372, 1025, 908, 827, 777, 733, 701 cm^{-1}; δ_H (300 MHz, $CDCl_3$) 7.72−7.52 (12H, m), 7.38 (2H, s), 7.30 (2H, t, J 7.5 Hz), 6.56 (2H, d, J 7.5 Hz), 2.33 (6H, s); δ_C (125 MHz, $CDCl_3$) 139.2, 136.9, 135.6, 135.5, 134.2, 134.1, 131.6, 130.1, 130.0, 129.2, 127.8, 127.7, 126.5, 125.6, 121.8, 20.2; *m/z* (CI) 433 $[M + H]^+$, 391, 307 (found: $[M + H]^+$, 433.1953. $C_{34}H_{24}$ requires $[M + H]^+$, 433.1956).

Synthesis of DSDPBF (11). The second half of the synthesis is provided in Scheme 2. To a suspension of compound (**8**; 87 mg, 0.201 mmol) and *N*-bromosuccinimide (73 mg, 0.412 mmol) in carbon tetrachloride (1.0 mL) was added benzoyl peroxide (3 mg, 0.012 mmol). The orange mixture was heated to reflux giving a dark orange colored solution containing some solid. After a total of 4 h at reflux, the reaction mixture was allowed to cool to room temperature, and the solid succinimide was filtered off, washing through with carbon tetrachloride (15 mL). The solvent was removed under reduced pressure giving an orange foam. Purification by flash column chromatography over silica gel (hexane−dichloromethane 25:1) afforded the dibromide **9** as a yellow solid (85 mg, 72%): ^{1}H NMR (300 MHz, $CDCl_3$) δ 7.80−7.67 (m, 8H), 7.64 (s, 2H), 7.60−7.50 (m, 4H), 7.34 (m, 2H), 6.61 (d, $J = 7.2$ Hz, 2H), 4.80 (s, 4H); ^{13}C NMR (75 MHz, $CDCl_3$) δ 138.0, 136.0, 135.4, 134.6, 133.5, 132.8, 129.9, 129.5, 129.3, 129.2, 128.2, 128.0, 127.8, 126.3, 122.6, 31.4; IR (film) 3054, 2920, 2850, 1595, 1488, 1440 cm^{-1}; LRCIMS *m/z* 591 ($M + H^+$, 36), 511 (100), 431 (26); HRCIMS *m/z* calcd for $C_{34}H_{22}Br_2$, $M + H^+$, 589.0166; found, 589.0126.

To sodium sulfide (262 mg, 1.092 mmol), dibromide (**9**; 358 mg, 0.606 mmol), and 4 Å molecular sieves under argon was added dry THF (7.0 mL). The mixture was stirred at ambient temperature for a further 24 h. The mixture was diluted with dichloromethane and filtered through Celite and then washed through with more dichloromethane. The solvent was removed under reduced pressure to afford a yellow solid. Purification by column chromatography over silica gel (hexane−dichloromethane 2:1) afforded the sulfide **10** as an orange-brown sticky solid (263 mg, 94%): ^{1}H NMR (300 MHz, $CDCl_3$) δ 7.75−7−65 (m, 8H), 7.56 (m, 4H), 7.49 (s, 2H), 7.32 (m, 2H), 6.57 (d, $J = 7.1$ Hz, 2H), 4.27 (s, 4H); ^{13}C NMR (75 MHz, $CDCl_3$) δ 37.3, 121.7, 122.1, 125.8, 126.1, 127.7, 127.8, 127.9, 128.1, 129.2, 129.3, 129.4, 129.4, 129.5, 129.7, 129.7, 129.8, 129.9, 130.0, 130.0, 138.8; IR (film) 3055, 2923, 2852, 1765, 1692, 1606, 1494, 1440, 1373, 1264 cm^{-1}; LRCIMS *m/z* 463 ($M + H^+$, 100); HRCIMS *m/z* calcd for $C_{34}H_{22}S$, $M + H^+$, 463.1520; found, 463.1501.

To a stirred solution of the sulfide **10** (69 mg, 0.149 mmol) in dry dichloromethane (1.5 mL) at 0 °C under argon was added, dropwise, peracetic acid (0.125 mL, 0.60 mmol, 32 wt % in acetic acid). When the addition was complete, the reaction was warmed to room temperature and stirred for a further 30 h. The reaction was quenched with saturated aqueous sodium hydrogen carbonate (20 mL) and extracted with dichloromethane (3 ×

15 mL), and the organic layer was dried ($MgSO_4$), filtered, and concentrated under reduced pressure to afford a brown solid. Purification by column chromatography over silica gel (dichloromethane−hexane 1:1) afforded the sulfone **11** as an orange-brown solid (27 mg, 52%): ^{1}H NMR (300 MHz, $CDCl_3$) δ 7.80−7.65 (m, 8H), 7.60−7.50 (m, 6H), 7.35 (m, 2H), 4.42 (s, 4H); ^{13}C NMR (75 MHz, $CDCl_3$) δ 56.7, 122.6, 124.1, 126.4, 127.9, 128.3, 128.7, 129.4, 129.9, 130.0, 132.7, 134.4, 135.6, 135.7, 136.0, 138.2; IR (film) 3055, 2982, 2924, 1594, 1480, 1441, 1321, 1131 cm^{-1}; LRCIMS *m*/*z* 495 (M + H$^+$, 100); HRCIMS *m*/*z* calcd for $C_{34}H_{22}SO_2$, M + H$^+$, 495.1419; found, 495.1419.

Results and Discussion

Absorption and Emission. Even though the sulfone group was added to facilitate further reactivity, we were more interested in evaluating how the addition of an electron-withdrawing group, such as sulfone, positioned one carbon atom away from the aromatic π system, affects the electrochemical, spectrochemical, and ECL properties of benzo[*k*]fluoranthene. Additionally, we also studied the synthetic intermediate, the dimethylated benzo[*k*]fluoranthene, to evaluate the effects of a weakly donating substituent on these same properties. On the basis of the optimized geometry from AM1 semiempirical calculations for DSDPBF (Figure 1),[4] very little molecular orbital overlap between the aromatic π system and the sulfone was observed because of the presence of the carbon sp^3 orbital that was between each moiety; therefore, one would expect very little change in the physical properties of this molecule when compared to the unsubstituted benzo[*k*]fluoranthene. Figure 2, parts a and b, shows the absorbance and fluorescence emission spectrum of a ~20uM solution of DMDPBF and DSDPBF in benzene. Both compounds exhibit relatively strong absorbance in the ultraviolet/blue region and a fairly intense fluorescence in the blue region. A small Stokes shift <10 nm indicates very little reorganization in both molecules upon excitation. Using diphenylanthracene (DPA) as a standard, the quantum efficiency of DMDPBF was 1.0, whereas the quantum efficiency of DSDPBF was 0.33.[4] The lower quantum efficiency for DSDPBF is most likely due to the presence of the electron-rich sulfone group. Previous fluorescence studies have shown that substituents containing heavy atoms enhance intersystem crossing from the singlet excited state, thus, decreasing emission and resulting in lower efficiencies.[6]

Both spectra in Figure 2 are similar to the absorbance and fluorescence spectra of the unsubstituted DPBF.[3] Although the peaks in the absorbance and fluorescence spectra of DMDPBF are shifted approximately 3−6 nm to longer wavelengths, the absorption and fluorescence peaks of DSDPBF occur at almost the same wavelengths as the unsubstituted compound. This suggests that, in the dimethyl substituted compound, hyperconjugation occurs between the hydrogen orbitals on one of the dimethyl groups and the aromatic π system of benzo[*k*]-fluoranthene.[7] This extension of the π system results in a slight decrease in the transition energy between the HOMO and LUMO of DMDPBF. The loss of this effect upon the addition of the electron withdrawing sulfone group suggests one of two possible scenarios, either the orientation of the methyl groups has been altered such that hyperconjugation can no longer occur or induction through the σ bonds counter-balances electron donation resulting in a compound that has properties more similar to the unsubstituted compound. AM1 semiempirical calculations, however, did not indicate any molecular orbital density overlap from the sulfone group to benzo[*k*]fluoranthene

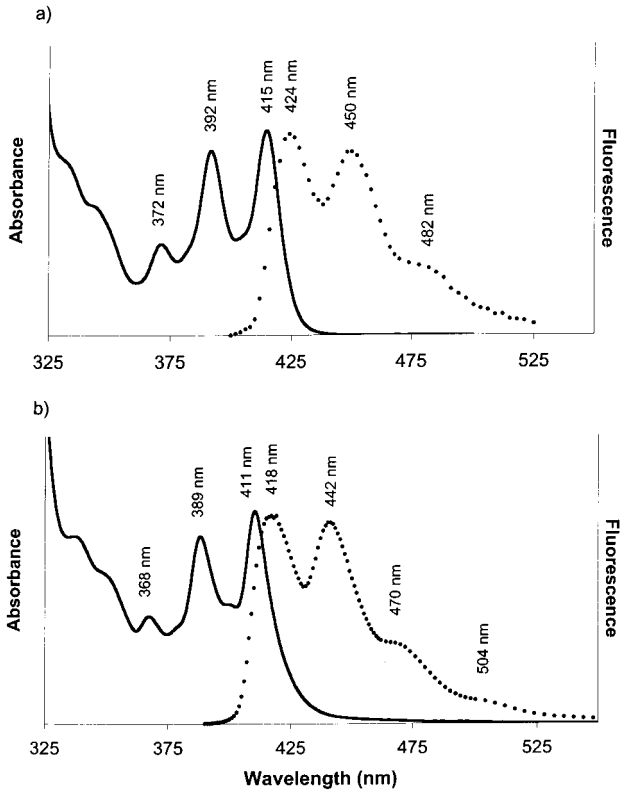

Figure 2. Absorbance (—) and fluorescence (···) spectrum of a 19.9 uM solution of DMDPBF (a) and DSDPBF (b) in benzene.

in either the HOMO or LUMO. This suggests that the addition of the sulfone group causes the hydrogen s orbital to rotate from the eclipsed conformation to a staggered conformation eliminating the overlap of this orbital with the π system required to produce hyperconjugation.[7]

Electrochemistry. As a result of the instability of the radical ions in the presence of water and oxygen, voltammograms of DMDPBF and DSDPBF were obtained in nonaqueous solvent mixtures that were prepared within an inert atmosphere drybox. Figure 3, parts a and b, shows cyclic voltammograms of both compounds obtained in 0.2 M TBAPF6 in 4:1 benzene/acetonitrile. The insets, included in both parts, are of scans taken with the switching potential set just past the first reduction wave. Both voltammograms exhibited electrochemical behavior that is similar to the previously studied unsubstituted monomer. At faster scan rates (υ > 1 V/s for DMDPBF and υ > 25 V/s for DSDPBF), the first oxidation wave was chemically reversible ($i_{pa}/i_{pc} = 1$) as long as the switching potentials were set prior to the onset of the second oxidation. The half wave potentials were 1.36 V vs SCE for DMDPBF and 1.5 V vs SCE for DSDPBF. Additionally, two reduction waves were observed; a chemically reversible wave ($i_{pc}/i_{pa} = 1$ at all υ) at a half-wave potential ($E_{1/2}$) of −1.95 V vs SCE for DMDPBF and −1.8 V vs SCE for DSDPBF and a chemically irreversible wave at a peak potential (E_p) of −2.5 V vs SCE for DMDPBF and −1.92 V vs SCE for DSDPBF. This irreversibility in the second reduction wave is most likely attributed to high reactivity of the radical dianion for residual protons in the electrolyte.[8] For the DSDPBF, however, the second reduction wave has a peak current that is considerably smaller than the peak current observed for the single electron transfer oxidation and the first reduction waves. Also, the peak separation between the first and second reduction waves is smaller than those for the other two benzo[*k*]fluoranthene derivatives. The peak current also decreased upon additional purification through column chro-

TABLE 1: Comparison between HOMO and LUMO Determined from AM1 Semiempirical Calculations and Voltammetic and Spectroscopic Data

fluoranthene derivative	$E_{p,oxid}$, (V) (V vs SCE)	$E_{p,red}$, (V) (V vs SCE)	ΔE_p, (V)	E_{S1-S0}, (V)	HOMO, (eV)	LUMO, (eV)	$\Delta E_{HOMO-LUMO}$
DPBF	1.60	−1.90	3.50	2.97	−8.183	−0.847	7.34
DMDPBF	1.35	−1.95	3.31	2.92	−8.110	−0.815	7.30
DSDPBF	1.60	−1.80	3.40	2.97	−8.428	−1.106	7.32

matography, suggesting that this wave may be associated with a difficult to remove impurity, possibly the harder to reduce bromonated intermediate, that is present in the final product.

As expected, the presence of the weak electron donating methyl groups facilitates radical cation formation lowering the oxidative peak potential from ∼1.6 V vs SCE for DPBF to 1.3 V vs SCE for DMDPBF. In the case of DSDPBF, the oxidation potential was about the same as that for DPBF ($E_{pa} \sim 1.6$ V vs SCE). As with the absorbance spectra, this effect could be attributed to the loss of hyperconjugation or the electron donating effect of the methyl groups upon addition of the sulfone groups. For the first reduction wave, no change in the potential was observed for DMDPBF; however, in the case of DSDPBF, the reduction wave shifted to more positive potentials from −1.90 V vs SCE for DPBF to −1.8 V vs SCE for DSDPBF. This indicates that the presence of the electron withdrawing sulfone group assists in the formation of the radical anion making it easier to reduce DSDPBF. Both voltammetry and spectroscopy show that the sulfone group influences the aromatic π system even though it is positioned one carbon atom away.

We were also interested in seeing if we could use semiempirical calculations to predict the physical behavior of the compounds studied in this investigation as well as future substituted benzo[*k*]fluoranthene derivatives. If a correlation could be derived between these calculations and the photophysical and electrochemical properties, then such calculations could be used to design future benzo[*k*]fluoranthene derivatives.

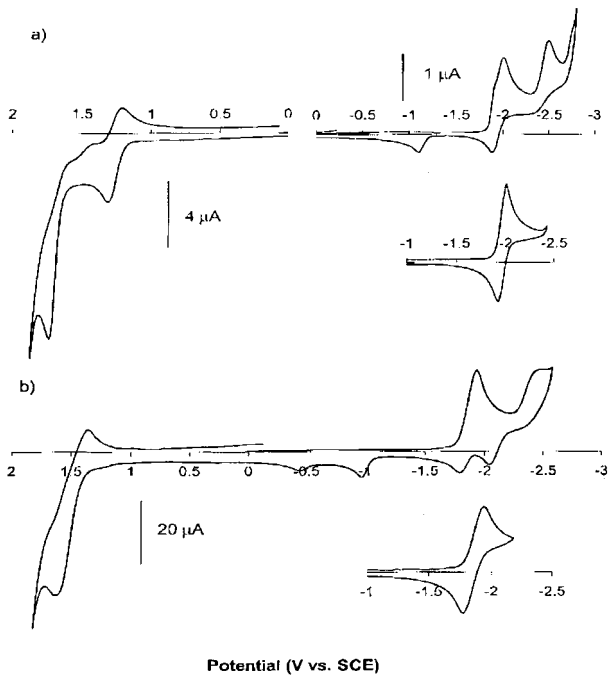

Figure 3. Cyclic voltammograms of a 2.2 mM solution of DMDPBF (a) in 0.1 M $TBAPF_6$ in 4:1 benzene/acetonitrile at a scan rate of 1 V/s (1 mm diameter Pt disk) and of a 2.2mM solution of DSDPBF (b) in the same electrolyte at a scan rate of 0.5 V/s (3 mm diameter Pt disk). Inserts: Scan taken with negative switching potential set just beyond the first reduction wave.

From the AM1 calculations that were already performed to determine the optimized structures of DPBF, DMDPBF, and DSDPBF, the calculated energy levels of the HOMO and LUMO of each compound were compared to the energy levels determined by the fluorescence and voltammetric data. These values are given in Table 1. Upon comparing the peak potentials for the oxidation and reduction to the calculated energy levels of the HOMOs and LUMOs, there appears to be a correlation between the reduction potentials and the energies of the LUMOs; however, a similar correlation could not be made for the oxidation potentials and the energies of the HOMOs. Additionally, a correlation could not be made between the energy difference between the ground state and the singlet excited state determined from the fluorescence spectra and the calculated energy difference. One possible reason for the lack of correlation may be the inability of the AM1 calculations to take into consideration either the hyperconjugation between the aromatic π system and the methyl groups substituted onto the 9,10 position of DMDPBF or the induction effect from the addition of the sulfone group to these methyl groups in DSDPBF. Presently, we are continuing our investigation into the use of more appropriate semiempirical calculations as a means of predicting future light emitting compounds.

As with the previously studied fluoranthene derivatives, RRC occurs upon electrochemical oxidation resulting in the formation of the deep red dimer.[3] The overall reaction scheme is given in Scheme 3 and through standard electrochemical terminology is an EC_2EECEE mechanism. Figures 4 and 5 illustrate the change in the shape of the oxidation wave of both compounds as a function of scan rate or reaction time. At faster scan rates

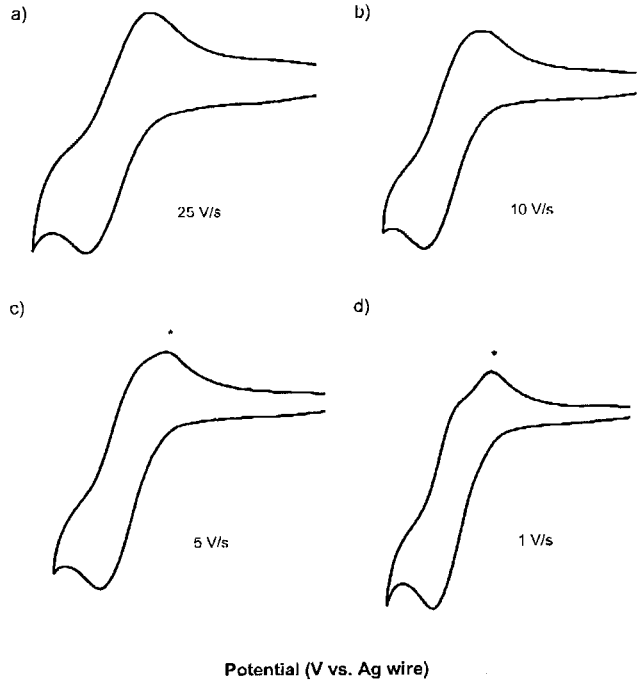

Figure 4. Cyclic voltammograms of 2 mM solution of DMDPBF in 0.1 M $TBAPF_6$ in 4:1 benzene/acetonitrile at scan rates of 1 (a), 0.1 (b), 0.05 (c), and 0.01 V/s (d).

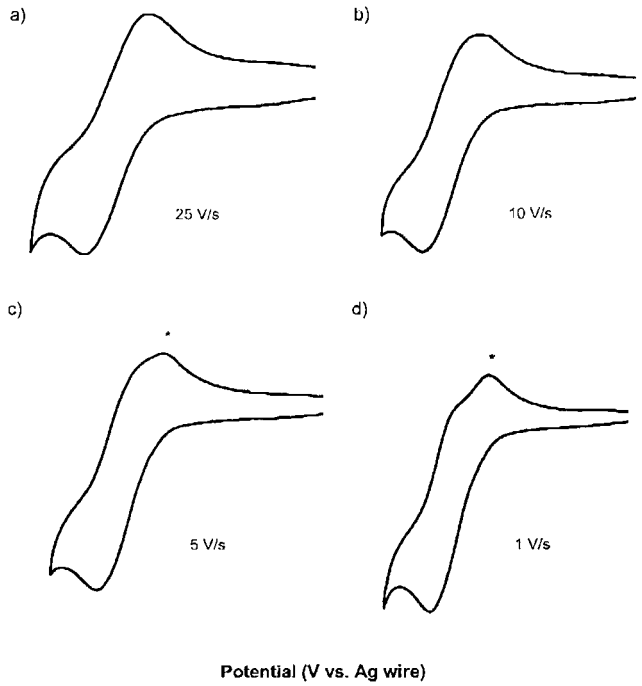

Figure 5. Cyclic voltammograms of a 2 mM solution of DSDPBF in 0.1 M $TBAPF_6$ in 4:1 benzene/acetonitrile at scan rates of 25 (a), 10 (b), 5 (c), and 1V/s (d).

(1 V/s for DMDPBF and 10 V/s for DSDPBF) or shorter reaction times, the oxidation wave is chemically reversible ($i_{pa}/i_{pc} = 1$), indicating very little formation of the dimer on this time scale; however, as reaction times are increased (scan rate decreased), this wave becomes irreversible ($i_{pa} > i_{pc}$), and a second reversible wave begins to appear at potentials different than the potential for monomer oxidation. Although the presence of oxidation waves associated with the dimethyl dimer is more difficult to observe in the voltammogram obtained at 0.01 V/s in Figure 4 because of the convection at this scan rate, presence of the dimer was confirmed by visually observing the formation of a red species in the vicinity of the electrode when biased 1.5 V and higher in potential. As with our previous studies, these waves can be attributed to one or more of the intermediates leading to the ladder dimer (Scheme 3). From the scan rate (υ), one can estimate the rate of dimerization through the use of the following equation: $k = (nF\upsilon)/(RT[M])$, where k is the reaction rate, n is the number of electrons involved in the heterogeneous electron transfer, υ is the scan rate at which the product is observed, $[M]$ is the concentration of the monomer, and F, R, and T are the corresponding constants.[9] By using this equation and the scan rate at which the dimer is first observed for both compounds, the rate of dimerization for DMDPBF was estimated to be 195 $M^{-1}s^{-1}$, whereas for DSDPBF, the rate was estimated to be 20 000 $M^{-1}s^{-1}$. These values are considerably different than the rate (7500 $M^{-1}s^{-1}$) observed for the unsubstituted benzo[*k*]fluoranthene and show the significant influence these substitutions have on the stability of the electrogenerated radical cation as well as chemical reactivity. Substitutions of electron donating groups directly onto aromatic moieties have been shown to stabilize the corresponding radical cation decreasing reactivity, whereas substitutions involving electron-withdrawing groups destabilize the radical cation increasing reactivity.[10] In our case, however, the electron-withdrawing sulfone is positioned one carbon away from the aromatic ring.

Bulk Electrolysis. To confirm that the dimer does indeed form upon electrochemical oxidation, bulk electrolysis was performed on 5 mM solutions of both compounds. A large area Pt mesh-working electrode was biased at the oxidative peak potential for 1 h in an attempt to generate significant amounts of the dimer needed for further characterization. During this period, the solution went from a pale yellow to a deep dark red color. A cyclic voltammogram of the resulting bulk electrolysis solution was obtained and is shown in Figure 6. The voltammogram contained a large number of overlapping oxidation and reductions peaks prior to the oxidation and reduction of the monomer, making it difficult to assign any of the peaks to the dimer; therefore, a sample of the electrolysis solution was removed from the inert atmosphere, and absorbance spectra were obtained. These are given in Figure 7. When compared to the spectra obtained in Figure 2, one can see the absorption bands associated with the monomer between 350 and 450 nm; however, new absorption peaks are now located between 475 and 650 nm. These longer wavelength bands confirm the presence of a new compound with a large increase in the aromatic π system or a higher degree of conjugation. The λ_{max} of each of the lower energy wavelength bands corresponds well to those previously measured for the unsubstituted dibenzotetraphenylperiflanthene dimer (490, 540, and 574 nm).[3]

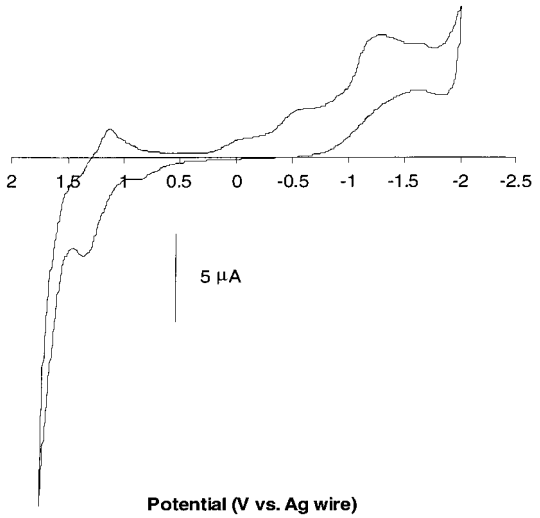

Figure 6. Cyclic voltammogram taken immediately after biasing a large area Pt mesh working electrode at 1.6V vs Ag wire for 1 h. The solution contained 5 mM DSDPBF. The voltammogram was obtained at a 1 mm Pt disk electrode at a scan rate of 0.2 V/s.

Though we were able to chemically synthesize and isolate the DMDPBF dimer, we were unable to isolate the DSDPBF dimer from the other products in the reaction solution.[3a] Figure 8 shows the absorbance and fluorescence spectrum and the cyclic voltammogram of the chemically synthesized and purified DMDPBF dimer. When the absorbance spectrum of the DMDPBF dimer is compared to the absorbance spectrum obtained for the electrolyte solution after bulk electrolysis, one can clearly see that the longer wavelength absorbance peaks are in fact due the presence of DMDPBF ladder dimer in solution. Additionally, we also tried to isolate the DSDPBF dimer from the final bulk electrolysis solution; however, after a 24 h period within the inert atmosphere box, the solution changed color going from a deep purple to a dark-brown. A second absorption spectrum was obtained and is shown in Figure 9 along with the spectrum taken 24 h earlier. In addition to a significant loss in the overall absorption intensity, the λ_{max} of the three dimer bands has shifted anywhere from 11 to 23 nm to longer wavelengths. Because, as Figure 8 shows, the resulting dimer undergoes oxidation at the potentials much lower than the oxidation of the monomer, this bathochromic shift in the absorbance may suggest additional

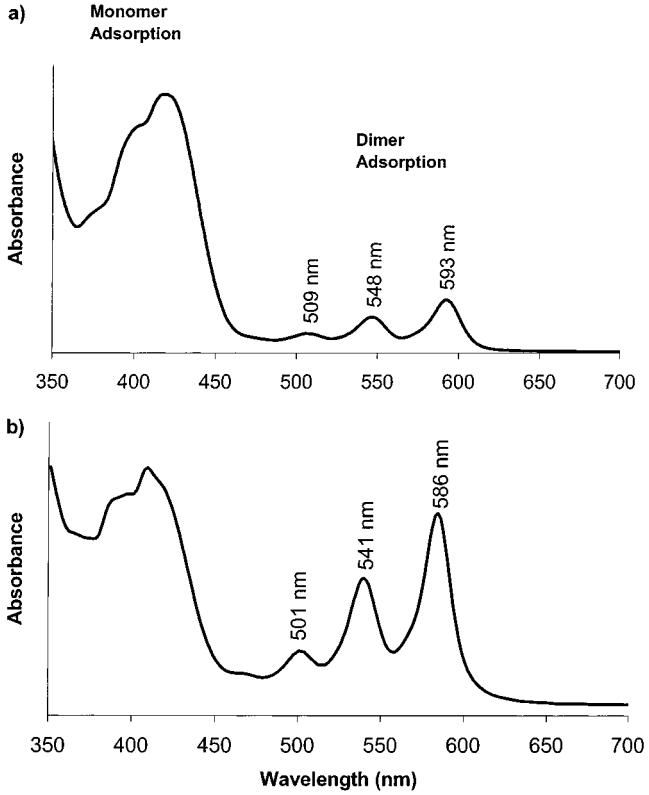

Figure 7. Absorbance spectrum of a 100-fold dilution of the bulk electrolysis solution of (a) DMDPBF and (b) DSDPBF after biasing the working electrode at 1.6 V vs QRE (Ag wire) for 1 h.

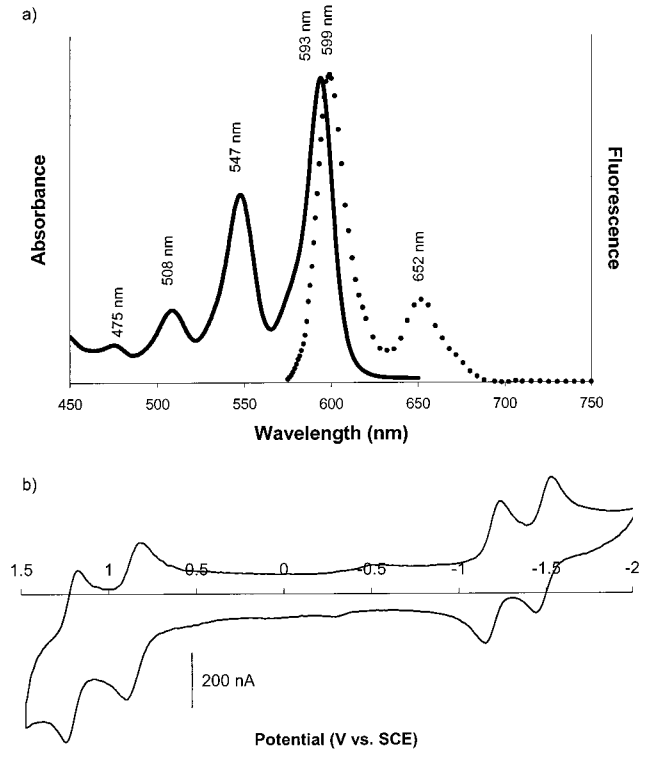

Figure 8. Absorbance spectra (a) of a 20 uM solution of the chemically oxidized DMDPBF ladder dimer and cyclic voltammogram (b) of a 0.5 mM solution of DMDPBF ladder dimer in 0.1 M $TBAPF_6$ in 4:1 benzene/acetonitrile.

couplings between the radical cations of the DSDPBF dimer and other oxidized species present in solution, which results in an even greater degree of conjugation. This chemical instability of the radical cation of the DSDPBF dimer may explain the inability to isolate the pure dimer upon chemical synthesis. Even though we were unable to identify the DSDPBF dimer through secondary elemental analysis, the absorbance spectrum in Figure 6b does confirm the formation of the ladder dimer upon electrochemical oxidation.

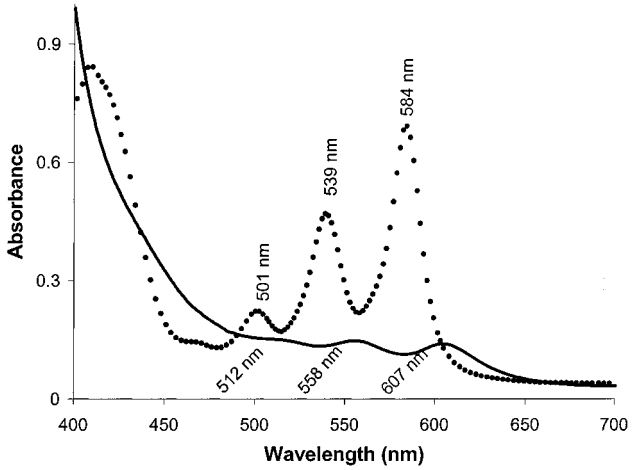

Figure 9. Absorption spectra of a 100-fold dilution of the bulk electrolysis solution of DSDPBF before (■) and after (—) 24 h in an inert atmosphere drybox.

Electrogenerated Chemiluminescence. With both compounds, the voltammetry shows that with careful control of the switching potential the electrochemical oxidation and reduction waves remain chemically reversible, therefore providing the stable radical ions needed to facilitate the electron transfer required to produce ECL. The total free energy of the annihilation reaction ($\Delta G_{ann} = \Delta H_s - T\Delta S$) can be estimated using the difference in the half-wave potentials of the oxidation and reduction waves in the cyclic voltammograms of DMDPBF ($\Delta E_{p(ox/red)} = 3.31$ V) and DSDPBF ($\Delta E_{p(ox/red)} = 3.30$ eV) given in Figure 3.[2c] This value, taking into consideration a ~ 0.1 eV loss in energy due to entropy ($-T\Delta S$), is 3.20 eV for both compounds. As calculated from the highest energy fluorescence at a λ_{max} of 417 nm, the energy needed to generate the excited state is 2.97 eV; therefore, the free energy of annihilation is more than sufficient to generate the singlet-excited state of DMDPBF and DSDPBF.

As a result of dimer formation upon electrochemical oxidation of the monomer, previous ECL measurements of the unsubstituted DPBF in unstirred solutions exhibited a moderate amount of dimer emission along with emission from the monomer. In stirred solutions, only monomer emission was observed in the ECL spectrum. Because the rate of dimerization for DMDPBF is considerably slower and the rate of dimerization for DSDPBF is considerably faster than the rate of dimerization for the unsubstituted DPBF, we would expect to observe significant differences in ECL emission of both compounds. Figure 10 shows the ECL emission spectrum of DMDPBF (a) and DSDPBF (b) measured upon pulsing the potential between the peak potentials of the first reduction and oxidation wave as the solution was stirred. As Figure 10 shows, the ECL spectrum of DMDPBF exhibited emission mostly from the monomer at 485 nm with a small amount of emission from the single sigma bonded dimer as is evident from the shoulder at ~580 nm. The ECL spectrum of DSDPBF contained emission from both the monomer at 487 nm and the dimers, single sigma bonded and double sigma bonded (see Scheme 3), at 589 and 621 nm. The DMDPBF dimer could be observed during ECL measurements by biasing the working electrode at the oxidative peak potential for 10 min prior to the ECL measurement (Figure 11). In

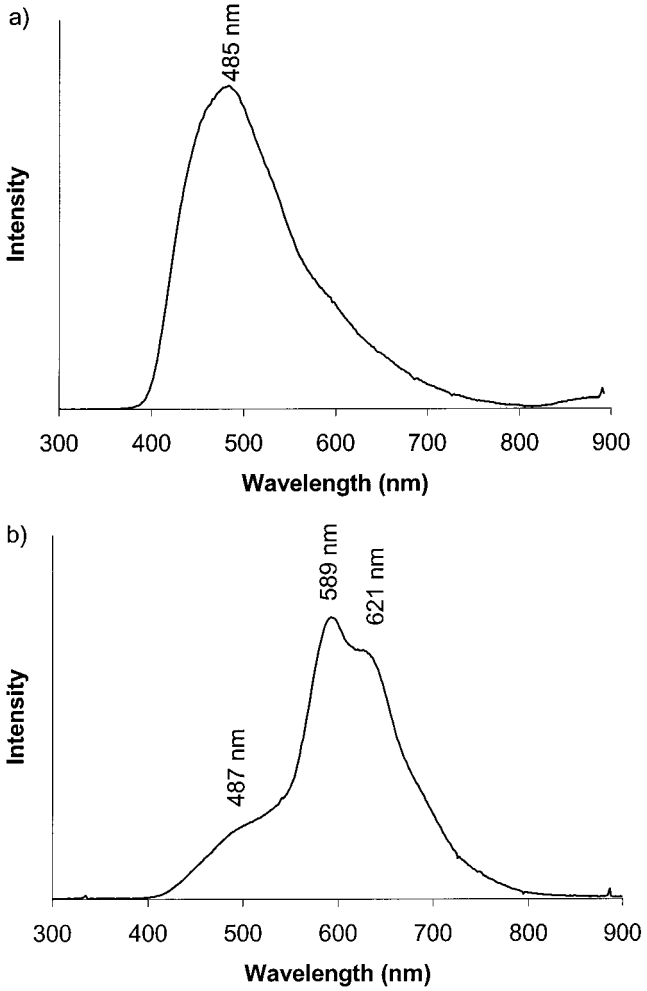

Figure 10. ECL emission from a 2 mM solution of DMDPBF (a) and DSDPBF (b) solution in 0.1 M $TBAPF_6$ in 4:1 benzene/acetonitrile obtained during pulsing between the oxidation and reduction peak potentials at a pulse width of 0.1 s.

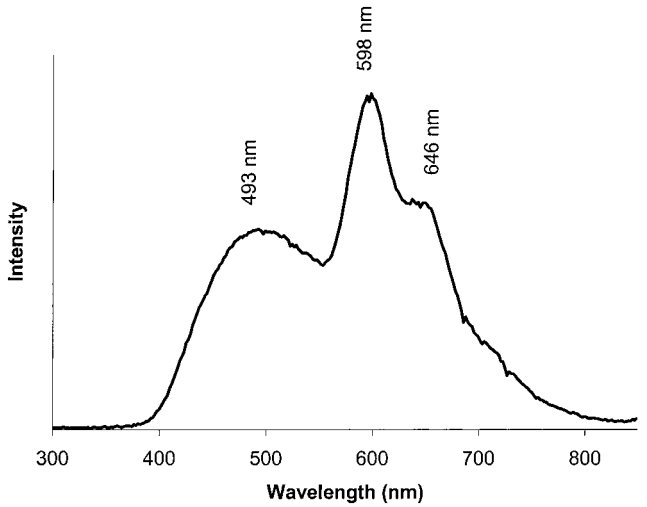

Figure 11. ECL emission spectrum of a 2 mM solution of DMDPBF in 0.1 M $TBAPF_6$ in 4:1 benzene/acetonitrile after biasing at 1.6V vs Ag wire for 10 min prior to pulsing between the oxidation and reduction peak potentials with a pulse width of 0.1 s.

addition to the monomer emission at 493 nm, emissions from both dimers are also observed at 598 and 649 nm. Under constant potential biasing, the reaction time was long enough to generate enough dimer in the vicinity of the electrode to result in emissions from these species. The ECL spectra, therefore, closely reflect the rate of dimerization for each of the benzo-[*k*]fluoranthene compounds studied. The relative ECL efficiency of DSDPBF was estimated to be twice ($\Phi = 0.10$) that of the ECL standard $Ru(bpy)_3ClO_4$ ($\Phi = 0.05$) showing the future potential of this compound for light emitting displays.[5]

Conclusions

Overall, the photochemical and electrochemical properties of DSDPBF were more similar to those of unsubstituted DPBF than those of DMDPBF; the only difference being a decrease in the quantum efficiency upon addition of the electron-rich sulfone group. The addition of the electron withdrawing sulfone group one carbon away from the main aromatic structure eliminates the hyperconjugation or back-donation of electrons from one of the hydrogen s orbitals of each methyl group observed in the dimethyl substituted monomer. These similarities were not observed in the rate of dimerization observed upon RRC upon electrochemical oxidation. The addition of the electron donating methyl groups decreased the stability of the radical cation, resulting in a rate of dimerization that was 40 times slower than that of the unsubstituted monomer. The subsequent addition of the electron withdrawing sulfone group increased the radical cation stability resulting in a rate of dimerization that was three times faster than that of the unsubstituted monomer. These results show that the presence of an electron-withdrawing group one carbon atom away from the aromatic core greatly influences the aromatic π system of the oxidized monomer resulting in a destabilization of the radical cation formed upon electrochemical oxidation. As a result, the ECL spectrum of DSDPBF was dominated by emissions from the dimer at 589 and 621 nm instead of the emission from the monomer at ca. 485 nm.

Acknowledgment. This research was supported by the Texas Advanced Research Program (ARP-190) and the Robert A. Welch Foundation. We also acknowledge Dr. Jeff Debad for his assistance.

References and Notes

(1) (a) Hercules, D. M. *Science* **1964**, *145*, 808. (b) Visco, R. E.; Chandross, E. A. *J. Am. Chem. Soc.* **1964**, *86*, 5350. (c) Santhanam, K. S. V.; Bard, A. J. *J. Am. Chem. Soc.* **1965**, *87*, 139.

(2) For reviews of ECL, see: (a) Faulkner, L. R.; Bard, A. J. *Electroanalytical Chemistry*; Bard, A. J., Ed.; Marcel Dekker: New York, 1977; Vol. 10, p 1. (b) Faulkner, L. R.; Glass, R. S. *Chemical and Biological Generation of Excited States*; Academic Press: New York, 1982; p 191. (c) Knight, A. W.; Greenway, G. M. *Analyst (Cambridge, U.K.)* **1994**, *119*, 879. (d) Knight, A. W. *Trends Anal. Chem.* **1999**, *18* (1), 47.

(3) (a) Debad, J. D.; Morris, J. C.; Lynch, V.; Magnus, P.; Bard, A J. *J. Am. Chem. Soc.* **1996**, *118*, 2374. (b) Debad, J. D.; Morris, J. S.; Magnus, P.; Bard, A. J. *J. Org. Chem.* **1997**, *62*, 530.

(4) (a) Stevens, B.; Algar, B. E. *J. Phys. Chem.* **1968**, *27* (7), 2582. (b) Morris, J. V.; Mahaney, M. A.; Huber, J. R. *J. Phys. Chem.* **1976**, *80*, 969. (c) Eaton, D. F. *Pure Appl. Chem.* **1988**, *60*, 1107.

(5) McCord, P.; Bard, A. J. *J. Electroanal. Chem.* **1991**, *318*, 91.

(6) (a) Christodouleas, N. D.; McGlynn, S. P. *J. Chem. Phys.* **1964**, *40*, 166. (b) Ramakrishman, V.; Sunseri, R.; McGlynn, S. P. *J. Phys. Chem.* **1962**, *37*, 1818. (c) McGlynn, S. P.; Daigre, J.; Smith, F. J. *J. Phys. Chem.* **1963**, *39*, 675. (d) McGlynn, S. P.; Azumi, T.; Kasha, M. *J. Phys. Chem.* **1964**, *40*, *507*.

(7) (a) Hehre, W. J.; Pople, J. A.; Devaquet, A. J. P. *J. Am. Chem. Soc.* **1976**, *98*, 664. (b) Pross, A.; Radom, L.; Riggs, N. V. *J. Am. Chem. Soc.* **1980**, *102*, 2253.

(8) *Encyclopedia of Electrochemistry of the Elements*; Bard, A. J., Ed.; Marcel Dekker: New York, 1978; Vol. 11, pp 105−114.

(9) (a) Yang, H.; Bard, A. J. *J. Electroanal. Chem.* **1991**, *306*, 87. (b) Yang, H.; Wipf, D. O.; Bard, A. J. *J. Electroanal. Chem.* **1992**, *331*, 913.

(10) Schmittel, M.; Burghart, A. *Angew. Chem., Int. Ed. Engl.* **1997**, *36*, 2550.